JOURNAL OF GEOPHYSICAL RESEARCH, VOL. 86, NO. B9, PAGES 7843–7854, SEPTEMBER 10, 1981

The Use of Height Data in Gravity Field Approximation by Collocation

RENÉ FORSBERG AND C. C. TSCHERNING

Geodetic Institute, Gamlehave Allé 22, DK-2920 Charlottenlund, Denmark

The accuracy of a gravity field model depends on the amount of available data and on the variation of the gravity field. When topographic height data are available, for example, in the form of a digital terrain model, it is possible to smooth the gravity field on a local scale by removing the gravitational effects calculated from models of the topographic masses. In this way, significant improvements of the prediction results are obtained in mountainous areas. In this paper we describe methods for the calculation of such gravitational terrain effects, applicable in collocation approximation of the gravity field. The terrain effects on gravity field quantities such as gravity anomalies, deflections of the vertical, and geoid undulations are calculated using a system of rectangular prisms, representing either a quasi-traditional model of the topography and the isostatic compensation or a residual terrain model, where only the deviation of the topography from a mean elevation surface is considered. To test the terrain reduction methods, numerical prediction experiments have been conducted in the mountainous White Sands area, New Mexico. From gravity anomalies spaced approximately 6 arc min apart, other known gravity anomalies and deflections of the vertical were predicted using collocation. When using terrain effects calculated on the basis of 0.5 × 0.5 arc min point heights, the rms errors decreased by a factor of nearly 3 to 1 arc sec for the deflections and 3–4 mGal for the gravity anomalies, quite insensitive to the actual type of terrain reduction used. The feasibility of using topographic reductions in collocation is thus effectively demonstrated.

1. INTRODUCTION

The object of gravity field prediction is to estimate unknown quantities related to the gravity field, e.g., deflections of the vertical, height anomalies (i.e., geoid undulations) and gravity anomalies. Typical applications of gravity field prediction include, e.g., estimation of geoid undulations in satellite-positioned geodetic stations (in order to convert the 'observed' ellipsoidal heights to heights above mean sea level), estimation of mean free air gravity anomalies from satellite altimeter data in oceanic areas and estimation of deflections of the vertical for use in the reduction of geodetic angle observations or in precise inertial navigation.

Traditional approaches, such as Stoke's and Vening-Meinesz' integral methods, basically use only one type of data in the prediction of another, e.g., the estimation of deflections of the vertical from a set of gravity anomalies. In many situations, there will, however, be available many different kinds of gravity field data, all containing significant gravity field information.

Such heterogeneous data can be fully utilized in the collocation approximation method by which one may construct an, in a sense, optimal approximation to the gravity potential using a given set of gravity field quantities, typically consisting of a set of spherical harmonic coefficients, 1° × 1° mean gravity anomalies, point observations of gravity anomalies, and deflections of the vertical. In the collocation method, each observation, regardless of the data type, is treated as the value of a functional applied on the anomalous potential, and some optimal 'smooth' least norm approximation is constructed in accordance with the observed functional values in a way such that the approximation is a harmonic function. The prediction results obtained using collocation depend, of course (as for all methods), on the available density of gravity field observations and the local gravity field variation. In mountainous areas a major part of this variation is due to the topography, a fact illustrated by the smoothness of the Bouguer anomalies versus the free air anomalies, the last being the type of gravity anomaly directly related to the anomalous potential. It is thus clear that in areas with rugged topography it will be advantageous to eliminate the effect of the terrain.

The local effect of the topography is also very marked on deflections of the vertical (easily contributing 10–20 arc sec) and on higher-order derivatives, whereas the local topographic effect on the geoid is relatively small, typically in the centimeter range under individual hills or mountains. On a more regional scale (hundreds of kilometers) the effects of the topography become very large, and in order to avoid biasing gravity and height anomalies, it is necessary to include the effect of the isostatic compensation, e.g., by the use of the Airy isostatic model, in which mountain masses are compensated by crustal roots, extending into the denser mantle, to secure local hydrostatic equilibrium. Alternatively, to the use of the isostatic compensation, one may choose only to take the 'short periodic' variations of the topography into account, removing the effect of the 'residual' topography with respect to some mean elevation surface. In this way the total mass removed will in the average sum to zero, as for the topographic/isostatic reduction.

In sections 3 and 4 of this paper we will describe practical methods and formulas for the calculation of the terrain effects on the commonmost gravity field quantities. We have chosen to use the prism method, where the influence of the terrain is calculated using rectangular prism integration elements. Most earlier papers dealing with this method are concerned with calculation of gravity terrain corrections, e.g., *Ehrismann et al.* [1966], *Boedecker* [1975], and many others. Applications for deflections of the vertical are reported by *Elmiger* [1969] and for height anomalies by *Gurtner* [1978].

The methods are tested and compared in a numerical prediction experiment with data from two 1° × 1° areas in New Mexico. The promising prediction results are presented in section 5. Let us, however, first give a brief description of the earth's gravity field and the method of collocation.

Paper number 1B0573
0148-0227/81/001B-0573$01.00

2. APPROXIMATION OF THE GRAVITY FIELD USING COLLOCATION

Let the gravity potential of the earth, W, be expressed as

$$W = U + T \tag{1}$$

where U is the normal potential, determined by the parameters of a chosen reference ellipsoid, and T is the anomalous potential. In U is included the centrifugal potential and the effects of all masses external to the earth, and thus T will be a harmonic function ($\nabla^2 T = 0$) outside the surface of the earth. As T is a small quantity compared to W, we will work with T in spherical approximation, where the earth is approximated by a sphere of radius $R = 6371$ km. We will also suppose that T can be developed as a series in solid spherical harmonics, i.e.,

$$T(\phi, \lambda, r) = \frac{GM}{r} \sum_{i=2}^{\infty} \left(\frac{R}{r}\right)^i \sum_{j=0}^{i} \bar{P}_{ij}(\sin\phi)(\bar{C}_{ij}\cos j\lambda + \bar{S}_{ij}\sin j\lambda) \tag{2}$$

where r is the distance from the origin (coincident with the earth's center of mass), ϕ and λ are the geocentric latitude and longitude, respectively, G the gravitational constant, M the mass of the earth, and $\bar{P}_{ij}$ are the fully normalized associated Legendre polynomials. Because T is a harmonic function, it will be an element of a reproducing kernel Hilbert space of harmonic functions. Such a space is a linear vector space with an inner product $(\cdot, \cdot)$ and a function $K(P, Q)$, the reproducing kernel, which is an element of the space itself if one of the variables are held fixed and which has the 'reproducing' property $f(P) = (f(Q), K(P, Q))$. For details see *Tscherning* [1978*a*] or *Moritz* [1980].

The observed gravity field quantities may be expressed as linearized functionals applied on the anomalous potential, $m_i = L_i(T)$. We have, e.g., for the most important quantities,

Height anomaly

$$\zeta = T/\gamma \tag{3}$$

Deflections of the vertical

$$\xi = -\frac{1}{r\gamma}\frac{\partial T}{\partial \phi} \tag{4}$$

$$\eta = -\frac{1}{r\cos\phi\,\gamma}\frac{\partial T}{\partial \lambda} \tag{5}$$

(Free air) gravity anomaly

$$\Delta g = -\frac{\partial T}{\partial r} - \frac{2}{r}T \tag{6}$$

where γ is the normal gravity. In so-called exact collocation a unique approximation $\tilde{T}$ to T is constructed by requiring the observations to be reproduced exactly and $\tilde{T}$ to have minimum norm, the norm being defined by the inner product of the Hilbert space. The approximation will be a linear combination of the harmonic functions $L_i K(\cdot, Q)$(the dot indicates that L_i has been applied on $K(P, Q)$ as a function of P):

$$\tilde{T}(Q) = \sum_i a_i L_i K(\cdot, Q) \tag{7}$$

where the coefficients a_i are determined by solving the normal equations

$$\{L_i L_j K(\cdot, \cdot)\}\{a_i\} = \{m_j\} \tag{8}$$

If the observations contain errors, the variance of the errors must be added to the diagonal elements of $\{L_i K_j K(\cdot, \cdot)\}$. In this case a weighted square sum of the norm of $\tilde{T}$ and the observation errors is minimized. For details, see, e.g., *Tscherning and Forsberg* [1978].

The norm of the Hilbert space is determined through the selection of a reproducing kernel K. For a rotational invariant inner product, K will have the form

$$K(P, Q) = \sum_{i=2}^{\infty} \sigma_i \left(\frac{R_b^2}{rr'}\right) P_i(\cos\psi) = K(r, r', \psi) \tag{9}$$

where σ_i are positive constants (the degree variances), R_b the radius of a sphere bounding the area of harmonicity (the Bjerhammar sphere), r and r' the distances from the origin of P and Q, respectively, and ψ the angular distance between P and Q. The series (9) may in many cases be represented by closed expressions, thus strongly facilitating the numerical evaluation of the quantities $L_i L_j K(\cdot, \cdot)$. When the σ_i are chosen to approximate the empirical degree variances,

$$\sigma_i \approx \sum_{j=0}^{i} (\bar{C}_{ij}^2 + \bar{S}_{ij}^2) \tag{10}$$

then K represents the empirical covariance function for the anomalous potential T. In this case the approximation technique is denoted least squares collocation, as the approximation $\tilde{T}$ fulfils a least squares principle [*Heiskanen and Moritz*, 1967]. (Note that T is not necessarily an element of the used Hilbert space. However, the only condition to be fulfilled in order to enable the construction of $\tilde{T}$ is that (8) can be solved.)

In this paper we have used the least squares collocation method for our test predictions in New Mexico. As degree variances, we used simple rational function expressions, resulting in a closed expression for K, as described in our earlier paper [*Tscherning and Forsberg*, 1978]. Through a choice of appropriate function constants, the overall shape of the reproducing kernel is designed to approximate the empirical covariance function, determined on the basis of the observation material. The actual approximations were produced in steps, each step taking into account information with frequencies up to higher and higher degrees (so-called 'stepwise collocation,' cf. *Tscherning* [1974]). In the first step we used a set of potential coefficients ($\bar{C}_{ij}$, $\bar{S}_{ij}$). Then a regional approximation was constructed using $1° \times 1°$ mean free air anomalies, and finally, a local approximation was produced using (a part of) the available point gravity field data (free air anomalies and deflections of the vertical).

3. TERRAIN REDUCTIONS IN COLLOCATION

The gravity field effect of the topography and (contingently) the isostatic compensation is adequately accounted for by a simple 'remove-restore' technique, where not T itself but

$$T^c = T - T_m \tag{11}$$

is approximated.

Here T_m is a potential generated by a mass model of the terrain. To secure that T^c will also be a (harmonic) potential, T_m must be the potential of a given fixed volume of mass, e.g., all 'terrain masses' in a given 'square' bounded by latitude parallels and meridians. Then T_m will be harmonic outside the terrain masses and T^c a harmonic function (the 'terrain-reduced' potential) outside both the surface of the earth and the mass model.

In the collocation process we are thus using 'reduced' observations:

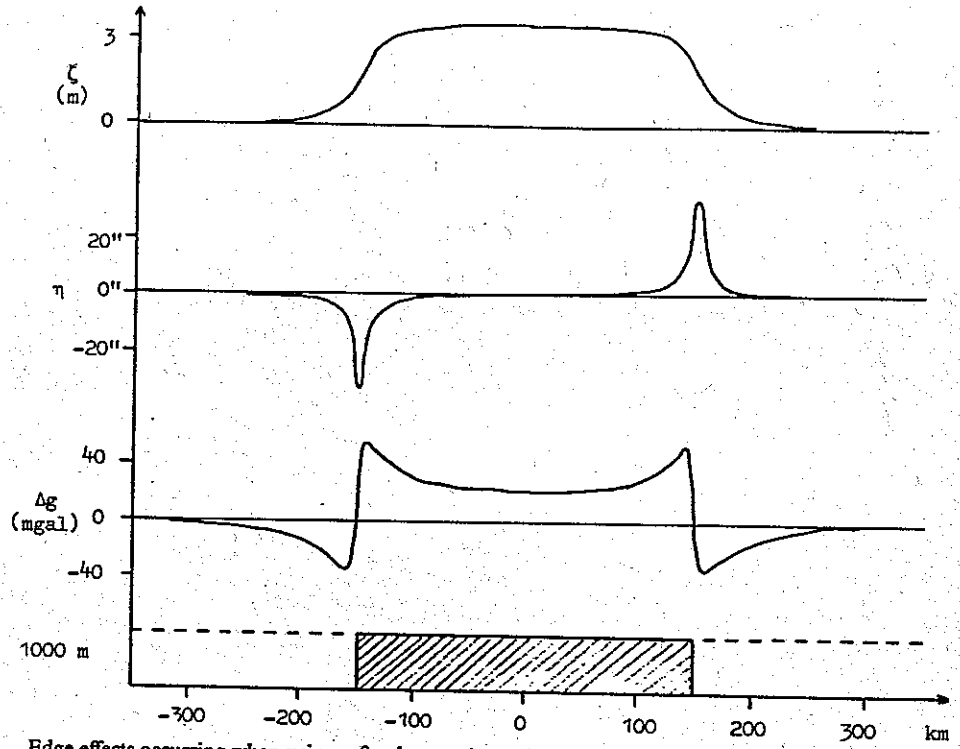

Fig. 1. Edge effects occurring when using a fixed-sector isostatic reduction. Figure shows quantities $L(T_m)$ in the central profile, when using a fixed 300 × 300 km sector for a topography with constant elevation 1000 m.

$$L_i^{obs}(T^c) = L_i^{obs}(T) - L_i^{obs}(T_m) \tag{12}$$

and get the final predictions by

$$L_j^{pred}(\bar{T}) = L_j^{pred}(\bar{T}^c) + L_j^{pred}(T_m) \tag{13}$$

In principle, T_m can be generated by arbitrary models of the terrain, but in general, we will expect the most smooth T^c when the most realistic height data and density distribution are used.

As 'terrain model' we can use the topography and the Airy-Heiskanen isostatic compensation. The isostatic residuals (isostatic gravity anomalies, topographic/isostatic-reduced deflections of the vertical, etc.) are known to be very smooth both on the local and global scale. For height anomalies the effects ζ_m due to the combined effect of the topography and the isostatic compensation are generally small in contrast to height anomalies $\zeta_m^{(TOPO)}$ calculated from the visible topography only. On a global scale, e.g., the variation of $\zeta_m^{(TOPO)}$ is several orders of magnitude larger than the actual variation of the geoid. Thus the isostatic reduction should always be preferred to the (often equally smoothing) alternative consisting of just removing the visual topography.

Furthermore the Airy-Heiskanen isostatic model is a realistic model of the earth's crust, easily allowing for additional modeling of known geological density anomalies, as, e.g., sedimentary basins. The actual choice of the isostatic compensation parameters (normal crustal thickness T (not to be confused with the anomalous potential) and crust/mantle density contrast $\Delta\rho$) is of minor importance when used for prediction. Conventionally, $T = 30$ km and $\Delta\rho = 0.6$ have been used, but values around $T = 33$ km and $\Delta\rho = 0.4$ are more close to the physical reality.

As mentioned a 'fixed' terrain mass model must be used to 'generate' T_m. This implies that it is not possible to use, e.g., topographic/isostatic effects calculated only out to a certain distance from the station (e.g., the Hayford zone O_2, 166.7 km), but one must either take the global topography into account or, alternatively, only account for a fixed area in the reduction process. The calculation of global isostatic reduced quantities is faciliated by various isostatic reduction maps [e.g., *Kärki et al.*, 1961] and by expansions in spherical harmonics of the topographic/isostatic reduction potential [e.g., *Lachapelle*, 1975]. However, for prediction in a local area (e.g., a 1° × 1° square) the influence of the distant topography is nearly constant, and therefore only a fixed area reduction should be necessary. The fixed area used should cover the area of prediction with an appropriate margin in order to avoid the possible 'edge effects' occuring when abruptly terminating a model with mean heights different from zero (Figure 1).

As an alternative to the isostatic reduction, we can use a residual terrain model (RTM), i.e., the deviations of the topography from a mean height surface, defined by a coarse mean height terrain grid (Figure 2) and a suitable interpolation pro-

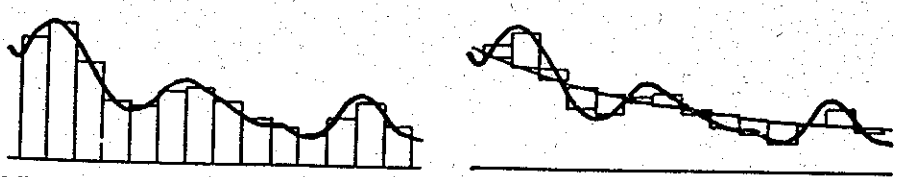

Fig.2. Modeling the topography (left) and the residual topography (right) with rectangular prisms. In the RTM reduction, masses above the mean elevation surface are removed, while valleys are filled (prism density negative).

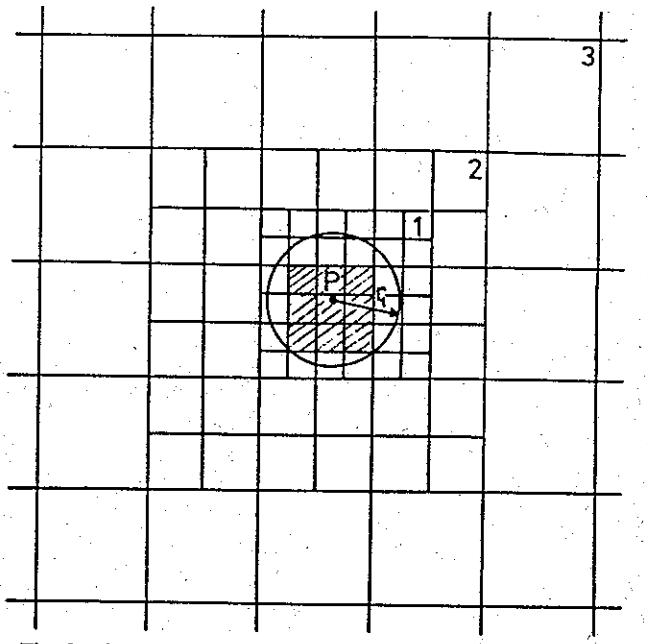

Fig. 3. Sectorization in the calculation of terrain effects. The hatched area is an example of an inner zone, where grid 1 is densified using a bicubic spline interpolation.

cedure, e.g., a simple bilinear interpolation. The 'coarseness' of the mean height grid should be decided on the basis of the density of observations and the local topography. The advantages of the RTM reduction compared to the isostatic reduction are significant computationally: there is no necessity for considering any isostatic compensation at all, and as the RTM have oscillating positive and negative densities (corresponding to the 'removal' of mountains and 'filling' of valleys), the effect of these will, in general, cancel out in a certain distance from the calculation point. Formally, we can thus operate with a global RTM without having to do the actual RTM reduction calculation out to more than a suitable distance from the calculation point. Moreover, as the formally global RTM consists of balanced positive and negative densities, the effects on 'long-wavelength' quantities such as, e.g., $1° \times 1°$ mean gravity anomalies and potential coefficients will virtually be negligible if the RTM is sufficiently short periodic, e.g., defined as the topographic irregularities relative to a (global) mean height surface of 10×10 arc min mean heights.

The drawback of the RTM reduction is that we reduce the area of harmonicity. A station situated in a valley (Figure 2) will after the reduction be situated inside the smoothed topography, bounded by the mean elevation surface. The observation is thus reduced to its actual values inside the mass, where the gravity potential is nonharmonic. To be able to use collocation, we will thus have to change the reduced observation to the value it would have, if the 'outer' potential was harmonically downward continuated to the observation point. We will term this correction of the reduced observations, which are situated below the mean elevation surface, the harmonic correction. Generally, this downward continuation of the outer potential is possible, as the mean elevation surface is very smooth and the density of the masses filling the valleys is known.

An approximate value for the harmonic correction can be found in the following way: consider a station situated Δh below the mean elevation surface. As this surface is smooth and nearly constant around the station, the masses between the level of the station and the mean elevation surface may nearly be viewed as a Bouguer plate. By condensing these masses in a mass plane just below the station, the potential outside the mean elevation surface is nearly left unchanged, but now the station will be situated outside the masses. The effect of this condensation will be nearly zero for height anomalies and deflections of the vertical, whereas gravity anomalies will decrease corresponding to the removal of a Bouguer plate above the station and insertion of a new (mass plane) below. The harmonic correction for gravity anomalies is thus $-4\pi G\rho\Delta h$, where ρ is the density of the 'fill-in' masses.

In the test predictions in New Mexico (section 5), both fixed-sector topographic/isostatic reduction and RTM reduction (with the simple harmonic correction) have been used, giving nearly the same results. The feasibility of the simple 'Bouguer' approach to the harmonic correction is thus demonstrated.

4. CALCULATION OF THE TERRAIN EFFECTS

Classically, terrain effects have been calculated using a subdivision of the calculation station surroundings in a series of concentric rings, each subdivided in a number of sectors, such as, e.g., the Hayford zones [*Hayford and Bowie,* 1912]. With an estimated mean height of a sector the contribution of the sector to the total terrain effect (possibly including the isostatic compensation) is easily calculated using the relatively simple formulas for the gravity field quantities at the axis of a cylindrical (or conical) segment.

For computerized calculations, with the topographic data given in the form of point or mean heights in a grid, it is convenient to retain the generally quasi-quadratic sector subdivision of the topography induced by the digital terrain model. The effect of a single sector must then be calculated using the more complex formulas for the gravity field quantities around a rectangular prism. To speed up the calculations and due to the fact that detailed height information generally only is necessary in the vicinity of the calculation point, it is adequate to use larger mean height sectors for the more remote topography. This principle is illustrated in Figure 3. In this paper we will term the subdivision pattern the sectorization. From the assumption that the area under consideration is covered by a sequence of digital terrain models with increasing sector sizes (and, ideally, the coarser height grids simply having been constructed by averaging the finer grids), we will characterize the sectorization by a series of calculation radii r_i. Each r_i represents the minimum distance out to which grid number 'i' must be utilized. In order to 'fill up' to the boundary in the next, coarser grid the average distance to the outermost calculation sectors of grid i will be somewhat larger that r_i, as seen from Figure 3. When the objective of the calculation is a reduction, taking masses in a given, fixed area into account, the sectorization principle can still be used, but now the effect of the last grid must be calculated precisely to the (often square) border of the reduction area.

It must be emphasized that the sectorization is only a calculation procedure aimed at speeding up the calculations and reducing the demand for detailed height information. The sectorization must be chosen in a way not to degrade seriously the accuracy of the calculation, as it (as mentioned in the previous section) is essential that the same physical mass model is used in all calculations for collocation.

To speed up the calculations further, it is possible to use simpler approximative formulas when summing up the contributions from the sectors, again with the same remark as for the sectorization: the approximation error must be small in order to reduce the 'terrain calculation noise' to a level preferably far below the accuracy of the later predictions. Owing to the sectorization, sectors far away from a calculation point will generally be represented by flat-topped prisms with a little height extent when compared with their sides, and the effects of such prisms are calculated approximately by the gravimetrical formulas of a horizontal mass plane through the prism center of mass, here termed the 'condensed' formulas. At this point, let us now collect the necessary exact and approximate formulas for the basic building element, the rectangular prisms of uniform density, for the most important gravimetric quantities.

Let the prism be situated as shown in Figure 4. We want to calculate a gravimetric quantity $L(T_m)$ at the origin. For the vertical component of gravity we get

$$\delta g_m' = -\frac{\partial T_m}{\partial z} = G\rho \int_{x_1}^{x_2}\int_{y_1}^{y_2}\int_{z_1}^{z_2} \frac{z}{r^3}\,dx\,dy\,dz \qquad (14)$$

$$r = (x^2 + y^2 + z^2)^{1/2}$$

where G is the gravitional constant and ρ the constant density of the prism. Integration gives [*Jung*, 1961]

$$\delta g_m = G\rho \left\{ \left\| x \log \frac{y + r_{z_2}}{x + r_{z_1}} + y \log \frac{x + r_{z_2}}{x + r_{z_1}} \right|_{x_1}^{x_2} \Bigg|_{y_1}^{y_2} - \left\| z \arctan \frac{xy}{zr} \right|_{x_1}^{x_2} \Bigg|_{y_1}^{y_2} \Bigg|_{z_1}^{z_2} \right\} \qquad (15)$$

Note that this expression is simply a sum over the eight corners of the prism, the individual corner terms often being cancelled by similar terms in adjoining neighbor prisms.

To get the condensed approximation formula, we have

$$\delta g_m' = G\kappa \int_{x_1}^{x_2}\int_{y_1}^{y_2} \frac{z_m}{r^3}\,dx\,dy \qquad (16)$$

$$z_m = \frac{z_1 + z_2}{2} \qquad r = (x^2 + y^2 + z_m^2)^{1/2}$$

where $\kappa = \rho(z_2 - z_1)$ is the surface mass density. Simple integration gives

$$\delta g_m = -G\kappa z_m \left\| \arctan \frac{xy}{z_m r} \right|_{x_1}^{x_2} \Bigg|_{y_1}^{y_2} \qquad (17)$$

Exact formulas for the deflections of the vertical are simply obtained by shifting the coordinate axes, so that (15) gives the horizontal gravity components: Let $\sigma g_m = \delta g_m(x_1, x_2, y_1, y_2, z_1, z_2)$. We then have

$$\xi_m = \frac{1}{\gamma}\,\delta g_m(z_1, z_2, x_1, x_2, y_1, y_2) \qquad (18)$$

$$\eta_m = \frac{1}{\gamma}\,\delta g_m(y_1, y_2, z_1, z_2, x_1, x_2) \qquad (19)$$

The condensed formulas can, of course, not be obtained this way, but simple integration gives

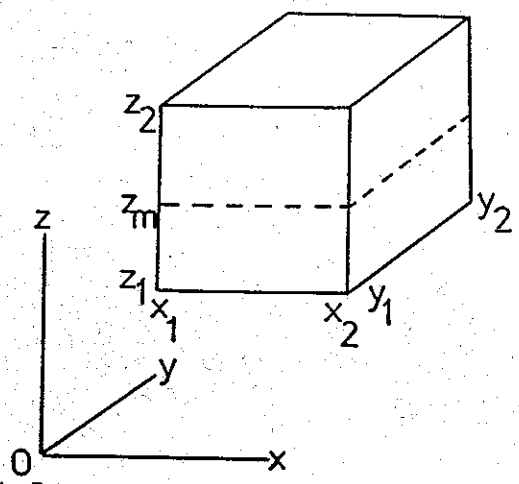

Fig. 4. Rectangular prism. In the condensed approximation the prism is replaced by the mass rectangle $z = z_m$.

$$\xi_m' = \frac{G\kappa}{\gamma} \left| \log \frac{x + r_{y_2}}{x + r_{y_1}} \right|_{x_1}^{x_2} \qquad (20)$$

$$\eta_m' = \frac{G\kappa}{\gamma} \left| \log \frac{y + r_{x_2}}{y + r_{x_1}} \right|_{y_1}^{y_2} \qquad (21)$$

The geoidal effect of a mass prism is simply derived from the potential by Bruns formula $\zeta_m = T_m/\gamma$. The exact formula, given by *MacMillan* [1958], contains a total of 36 log or arctan terms. It will not be shown here, as our testing of this formula against the condensed formula have shown that for all practical purposes the condensation approximation error is negligible, being typically only in the millimeter range for mountainous areas with 1000 to 2000 m mountains.

The condensed potential formula is derived from

$$T_m' = G\kappa \int_{x_1}^{x_2}\int_{y_1}^{y_2} \frac{1}{r}\,dx\,dy \qquad (22)$$

A similar integral is obtained when (14) is integrated one time with respect to z, and we therefore similarly get

$$T_m' = G\kappa \left\| x \log (y + r) + y \log (x + r) - z_m \arctan \frac{xy}{z_m r} \right|_{x_1}^{x_2} \Bigg|_{y_1}^{y_2} \qquad (23)$$

Owing to the relative insensitivity of the geoid to local topographic variations, it is often sufficient to use the simplest approximation formula for the potential, regarding the prism as a sphere having the mass of the prism. This especially is the case when evaluating the second (indirect) term of the free air anomaly expression

$$\Delta g_m = -\frac{\partial T_m}{\partial z} - \frac{2}{r}\,T_m \qquad (24)$$

where the first term is dominating except on a global scale.

In order to study the errors occurring when approximating the rigorous prism formulas with the corresponding mass plane formulas, consider a station P, situated in height H at a distance r from the center of a square sector with side length s and topographic height h (Figure 5). The relative approximation error for the gravity, the radial component of the deflection, and the height anomaly generally attains its maximal value for $H = h/2$ and when a prism corner is oriented toward P. However, with the typical flat-topped prisms in the distant sectors in the terrain calculations the approximation error is

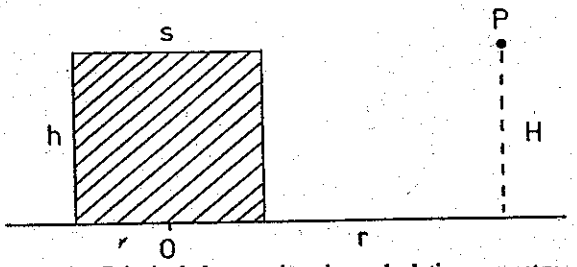

Fig. 5. Principal elements in prism calculation geometry.

roughly the same in all directions and for all heights H in the range zero to h. The relative approximation error is therefore primarily determined by the two dimensionless parameters r/s and h/s. Error curves for P situated centrally perpendicular to a side and in height $H = 0$ (or $H = 1$) are shown in Figure 6. With a given acceptable error and prism geometry (h/s) a minimum distance to which exact calculation formulas must be used is easily obtained.

Let us now return to the sectorization, in principle, the choice of sector size s versus the distance r to the computation point. In order to optimize the calculation the contribution from each sector should be of the same order of magnitude, of course under the restriction that the sectors must not be so big so that the constant height approximation of the sector topography becomes invalid. Let us consider a simple example where we want to calculate the total effect of the topography above sea level in the case of an altiplano with average height h. Consider a sector in distance r with side length s. We will then in a first approximation have

$$T_m \propto \frac{1}{r} s^2$$

$$\epsilon_m \propto \frac{1}{r^2} s^2 \tag{25}$$

$$\delta g_m \propto \frac{h}{r^3} s^2$$

where ϵ_m is the radial deflection component. In order to get equal effect proportional sector we must then have

$$T_m : s \propto r^{1/2}$$

$$\epsilon_m : s \propto r \tag{26}$$

$$\delta g_m : s \propto r^{3/2}$$

as shown in Figure 7, together with the conventional Hayford and Hammer zones primarily used in gravity terrain corrections. The above equal effect gravity sectorization results in very large distant sectors, which, of course, should be avoided. Our experience have shown us that in nearly all types of terrain effect calculations the classical $s \propto r$ sectorization is practical and gives good results. When using the earlier mentioned sequence of coarser and coarser height grids (Figure 3), a chosen r/s ratio is simply used to give the minimum distance r_i, to which grid i must be used. Note that a $r \propto s$ sectorization corresponds to a horizontal line in the approximation error graphs (Figure 6). For the quasi-Hayford $r/s = 1.5$ we see from the figure that the 1% error level is obtained for $h/s = 0.2$ and $h/s = 0.4$ for gravity and deflection, respectively. Hence the mass plane approximation can be used with an error of less than 1% from distances of around 5 h and 2.5 h, respectively. In our computations of terrain effects on gravity and deflections in New Mexico, described in the next section, we tested sectorizations with r/s in the range 1.2 to 4. Values around 1.6 proved to be sufficient [*Forsberg*, 1980].

Up to now we have implicitly presupposed the flat earth approximation. To account for the curvature of the earth we have two alternatives: either simply to 'suppress' the prisms the superelevation $\Delta z = r^2/2R$ below the horizon, retaining parallel prisms or, as is the only possibility in global calculations, let the prisms be oriented along the local meridian and vertical. In this case one has to calculate the complete attraction vector in the evaluation point P and subject it to an orthogonal transformation in order to get either the gravity or deflection components in P. This, of course, significantly increases the calculation time for cases where only one of the quantities is wanted. Formulas can be found from *Ehrismann et al.* [1966] (only gravity) or *Forsberg* [1980], including the spherical effects on the isostatic compensation. In our calculations in New Mexico, which covered at most a 6° × 7° area, the first alternative (parallel suppressed prisms) proved to be satisfactory.

In many approximation methods, such as stepwise collocation, a spherical harmonic expansion is used as a first approximation to the gravity potential. We therefore also need formulas for calculating terrain effects on potential coefficients. Consider a mass prism of density ρ at latitude ϕ and longitude λ, extending $\Delta\phi$ and $\Delta\lambda$ between heights h_1 and h_2, respectively. Let the anomalous potential be expressed in fully nor-

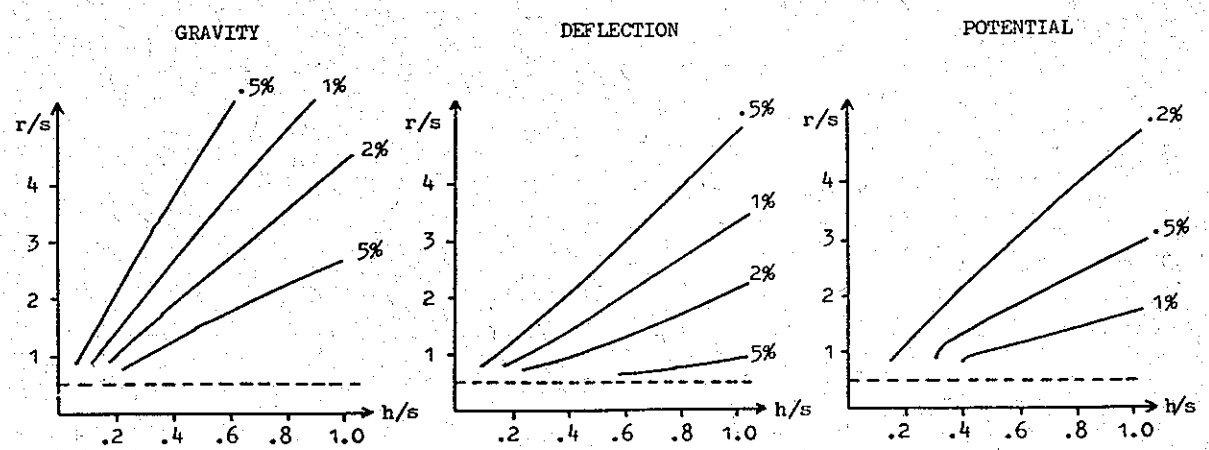

Fig. 6. Error curves for the relative approximation error, exact versus condensed prism formula, $H = 0$, central symmetry profile.

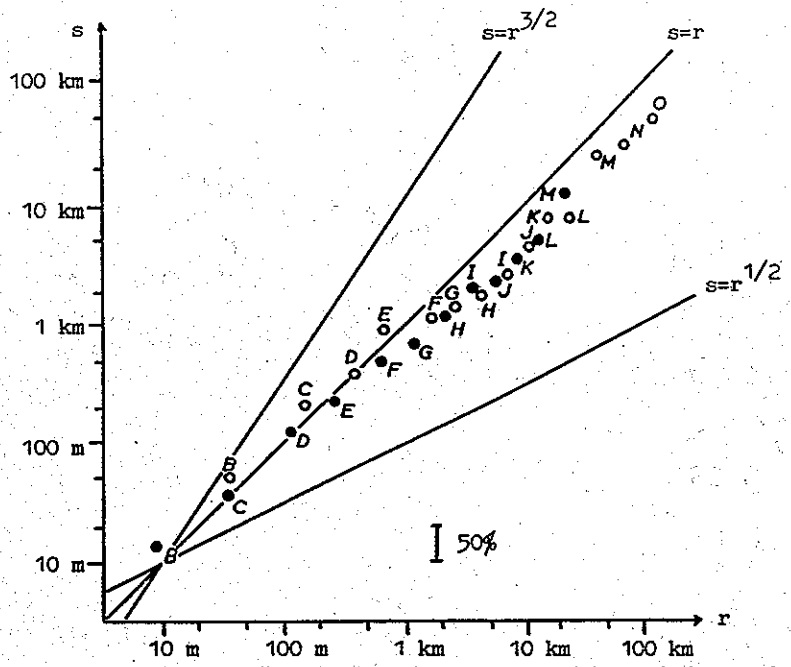

Fig. 7. Average side length s and mean radius r for the cylindrical sectors of the Hayford (open circles) and Hammer (solid circles) zone systems, [*Hayford and Bowie*, 1912; *Hammer*, 1939].

malized spherical harmonics, cf. (2). The coefficients of the expansion are given by

$$\left.\begin{matrix}\bar{C}_{ij}\\ \bar{S}_{ij}\end{matrix}\right\} = \frac{1}{(2i+1)MR^i}\int r^i \bar{P}_{ij}(\sin\phi')\left\{\begin{matrix}\cos m\lambda'\\ \sin m\lambda'\end{matrix}\right\}\Delta\rho\, dV \qquad (27)$$

where $\Delta\rho$ is some density distribution of the earth generating the anomalous potential [see, e.g., *Heiskanen and Moritz*, 1967]. For the mass prism contribution we get [*Lachapelle*, 1975]

$$\left.\begin{matrix}\bar{C}_{ij}^m\\ \bar{S}_{ij}^m\end{matrix}\right\} = \frac{1}{(2i+1)MR^i}\int_{\text{prism}} \rho r^i \bar{P}_{ij}(\sin\phi') \cdot \left\{\begin{matrix}\cos m\lambda'\\ \sin m\lambda'\end{matrix}\right\} r^2\cos\phi'\, d\phi'\, d\lambda'\, dh \qquad (28)$$

$$\left.\begin{matrix}\bar{C}_{ij}^m\\ \bar{S}_{ij}^m\end{matrix}\right\} \approx \frac{\rho}{(2i+1)MR^i}\bar{P}_{ij}(\sin\phi)\left\{\begin{matrix}\cos m\lambda\\ \sin m\lambda\end{matrix}\right\} \cdot \cos\phi\,\Delta\phi\,\Delta\lambda\int_{R+h_1}^{R+h_2} r^{i+2}\, dr \qquad (29)$$

$$\left.\begin{matrix}\bar{C}_{ij}^m\\ \bar{S}_{ij}^m\end{matrix}\right\} = \frac{\rho}{(2i+1)(i+3)MR^i}\bar{P}_{ij}(\sin\phi)\left\{\begin{matrix}\cos m\lambda\\ \sin m\lambda\end{matrix}\right\} \cdot \cos\phi\,\Delta\phi\,\Delta\lambda\,((R+h_2)^{i+3} - (R+h_1)^{i+3} \qquad (30)$$

due to the slow variation of the integrand over the relatively small $(\Delta\phi, \Delta\lambda)$ sector. In RTM reductions and fixed-area isostatic calculations with reduction areas of less than 5° × 5° we have found completely negligible potential coefficients for degree and order up to 36. This is, of course, not the case for global isostatic reductions, where the effect on all coefficients is significant [see, e.g., *Lachapelle*, 1975].

Finally, we consider the effect of the local station surroundings, say closer than 1 km to the station. This local effect is often very big for gravity anomalies and deflections. Around the calculation station we densify the finest digital terrain model using bicubic spline interpolation, but still there will always be a discrepancy between the station height (supposed to be on the ground) and the interpolated terrain model height. We have either to move the station up/down to the model 'ground' or to modify the terrain model in order to force it to give the correct height at the station. Numerical experiments using the data from New Mexico have shown that the first principle can be used for deflections and height anomalies. The gravity effects must always be calculated by modifying the terrain model (e.g., by some additional constant in an inner zone), as the effect is highly correlated with the station height, the 'discrepancy error' to a first order being simply the Bouguer term $2\pi G\rho\Delta h$.

5. Prediction of Deflections of the Vertical and Gravity Anomalies in the White Sands Area of New Mexico

The various terrain reduction methods were tested in two mountainous 1° × 1° areas in New Mexico, where known deflections of the vertical and gravity anomalies were predicted from (primarily) a set of gravity anomalies, spaced ca. 10 km apart, using the method of stepwise collocation implemented as described by *Tscherning* [1978*b*]. All data were transformed to the 'geocentric' reference system WGS 72. As height data 0.5 × 0.5 arc min point heights were used, and the calculation grid sequence was constructed from this detailed digital terrain model by using simple averaging. All data were kindly put to our disposal by the national Geodetic Survey, which also provided us with a datum shift NAD 1927 to WGS 72 valid for the White Sands area.

The two test areas are situated between latitude 32° to 34°N and longitude 107° to 106°W. Both areas are characterized by a N-S trending mountain chain, the Organ and San Andres Mountains, rising 800–1500 m above the surrounding plateau in a height of 1200–1400 m (Figure 8). To the east and west of the areas, higher mountains are rising. Geologically, the areas consist primarily of young Mesozoic sediments

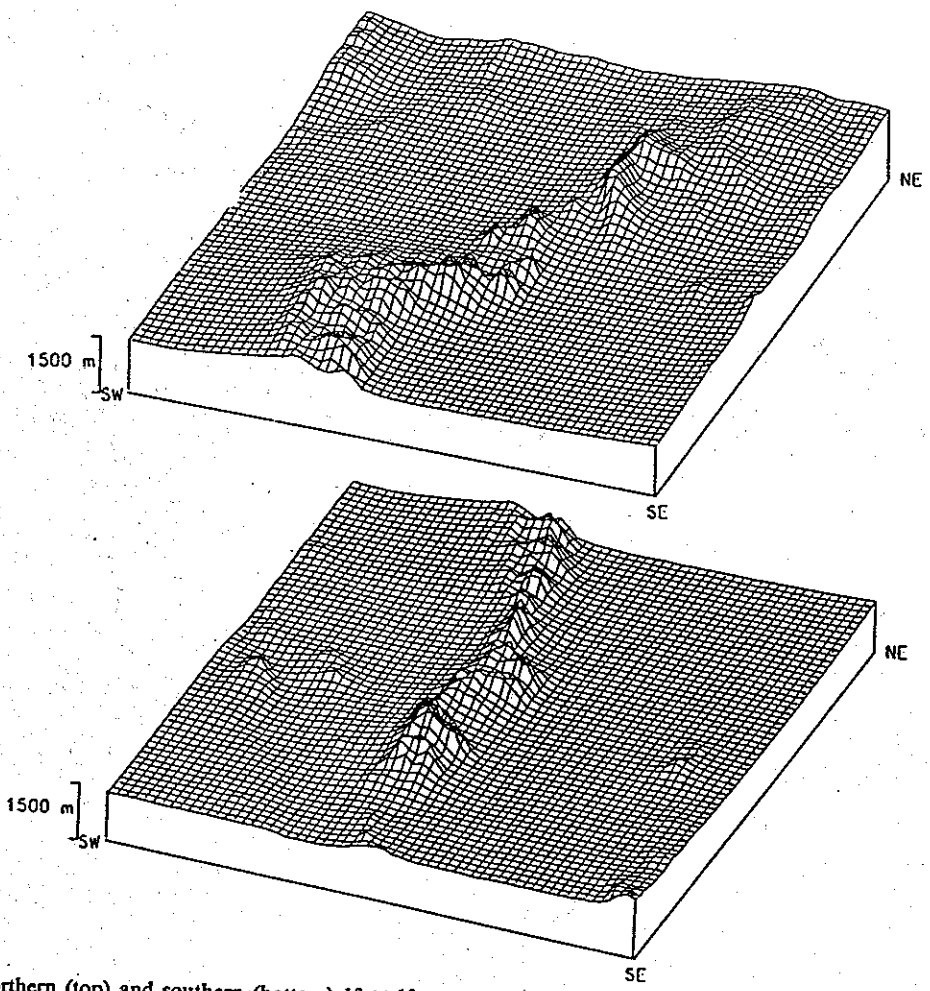

Fig. 8. Northern (top) and southern (bottom) 1° × 1° test areas, 32° to 34°N, 107° to 106°W; 1 × 1 arc min mean heights.

with some late Tertiary volcanics. *Woolard* [1962] indicates formation densities in the range 2.57–2.69 g/cm³ for the sediments, and it thus seems that the standard density 2.67 g/cm³ is a reasonable reduction density. We have used this value throughout. Observed point deflections of the vertical and gravity anomalies were predicted using stepwise collocation. As a first step, the GEM 10B spherical harmonic coefficient set was used, and as second step a set of 1° × 1° mean gravity anomalies was used. In the last step a local approximation was constructed using gravity anomalies spaced ca. 10 km apart, in some cases supplemented by a few deflections (40 km apart). The distribution of the gravity and deflection stations is shown in Figures 9 and 10. In each block, roughly 100 gravity anomalies are used in the prediction. The stepwise collocation prediction was performed analogously to our earlier investigations [*Tscherning and Forsberg*, 1978]. For the last prediction step, local empirical covariance functions were estimated for both gravity and deflections and subsequently used when choosing the reproducing kernel K to be used in the computations.

The predictions were performed with the original data as well as with data reduced for the influence of the terrain according to the various methods described in sections 3 and 4. The reductions treated in the following will be abbreviated as follows:

ISO fixed-sector topographic/isostatic reduction for a 6° × 7° area surrounding the test areas; Airy isostasy with crustal thickness 32 km and density contrast 0.4 g/cm³ is used;

TOPO fixed-sector (6° × 7°) reduction for the visible topography above sea level (thus, except for the fixed sector, corresponding to the classical 'refined' Bouguer correction with terrain correction);

RTM30 RTM reduction with the mean topography defined by a bilinear interpolation scheme in a 30 × 30 arc min mean height grid; residual topography in a fixed 3° × 4° sector taken into account;

RTM15 RTM reduction with 15 × 15 arc min mean height grid; only residual topography out to a distance of 60 km is taken into account.

Both the point observations and the mean gravity anomalies were terrain-reduced according to the chosen principle. As expected, the RTM effects on the mean gravity anomalies proved to be very small. ISO-reduced deflections of the vertical are shown in Figure 10, and Table 1 gives a survey of the statistics of the original and terrain-reduced observations for the combined area. From the table it is seen that the major part of the variation in the observed deflections and free air anomalies is due to the effect of the isostatically compensated topography. The actual choice of isostatic parameters proved to be of little importance in relation to the variation, but some isostatic effect should always be included to avoid the bias in

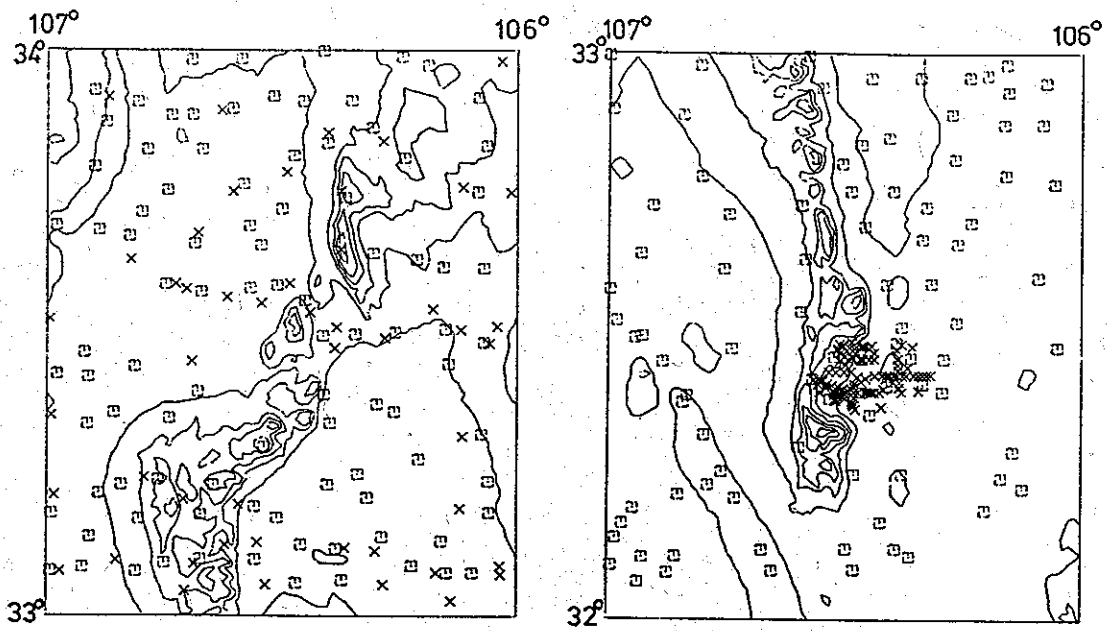

Fig. 9. Distribution of free air anomalies. Squares indicate data used in the prediction, crosses show comparison stations, where predicted values are compared to the observations. Topographic heights shown with 200-m contour interval.

the gravity anomalies (and height anomalies, too) occurring when only removing the topography (TOPO, Table 1). For the RTM reductions the variation is seen to increase when a finer height reference model is chosen, in correspondence with the fact that the RTM reduction only takes into account topographic variations with shorter 'periods' than the reference model mesh size.

Table 2 shows the combined results of the prediction in the two areas. A total of 110 deflection pairs and 150 gravity (free air) anomalies were predicted and compared to the known values. In column 'A' a total of 192 gravity anomalies and 18 deflection pairs were used as observations in the last collocation step, column 'B' shows the results obtained when omitting the deflections, and finally, column 'C' shows our results when only the 1° × 1° mean anomalies and GEM 10B are used as gravity field data. From the table it is clear that a remarkable improvement in the collocation prediction results occurs when the effect of the terrain is taken into account. The prediction rms error decreases with a factor of nearly 3 for both gravity and deflections when terrain-corrected data are used. The role of the topography is further illustrated by observing that we get better deflection prediction results using the ISO reduction without any local gravity information ('C') than by using all our gravity field data in the traditional collocation prediction neglecting the topography! (Investigations by *Fischer and Wyatt* [1974] in the Pacific Ocean further confirm that excellent deflection prediction results may be obtained solely based on topographic information.)

The RTM reductions are seen to give results equally as good as the topographic/isostatic reduction, and this supports both the simple 'harmonic correction,' introduced in section 3 and the suggestion that the reduction may be calculated only out to a fixed distance from the station without violating the harmonicity. When no local gravity data are present ('C'), the RTM reductions, of course, give poorer predictions than the complete topographic/isostatic reduction, again due to the fact that only a part of the topographic 'signal' is taken into account.

From Table 3 the very small influence of the isostatic parameters in the prediction is seen clearly. Note that the omission of any compensating masses only degrades the results slightly. This is quite remarkable in view of the biased gravity anomalies (Table 1).

Finally, Table 3 shows the ISO prediction results when a 5 × 5 arc min mean height grid (ca. 9 × 8 km sector size) is used as the most detailed digital terrain model. Deflection results are most markedly degraded but are still much better than the results obtained if the topographic information is neglected altogether. For the gravity stations the results are remarkably good. It must be remembered that we modified the terrain model to give the correct gravity station height, so the reason for the only slight improvement of prediction results seen when using detailed topographic information is that the simple Bouguer correction generally is a good approximation to the gravity effect of the topography. The approximation error (the gravimetric terrain correction) is generally small in comparison to the Bouguer correction itself, but it is well-known that it might be very large at stations with extreme locations and that very detailed height information is necessary for its evaluation. One should therefore always use the most detailed digital terrain models available when terrain reducing the gravity anomalies.

Other authors have in recent years published results of deflection predicexperiments in the White Sands area. Although comparisons of results are nearly impossible due to the different data involved, a short survey is presented in Table 4. It seems that stepwise collocation plus terrain reduction gives very good results.

6. CONCLUSIONS

Above we have described some practical methods by which topographic information in the form of digital terrain models can be used in a way consistent with gravity field approximation methods such as collocation. A very significant reduction of the prediction error occurs when accounting for the effect of the terrain in mountainous areas. Our investigations in

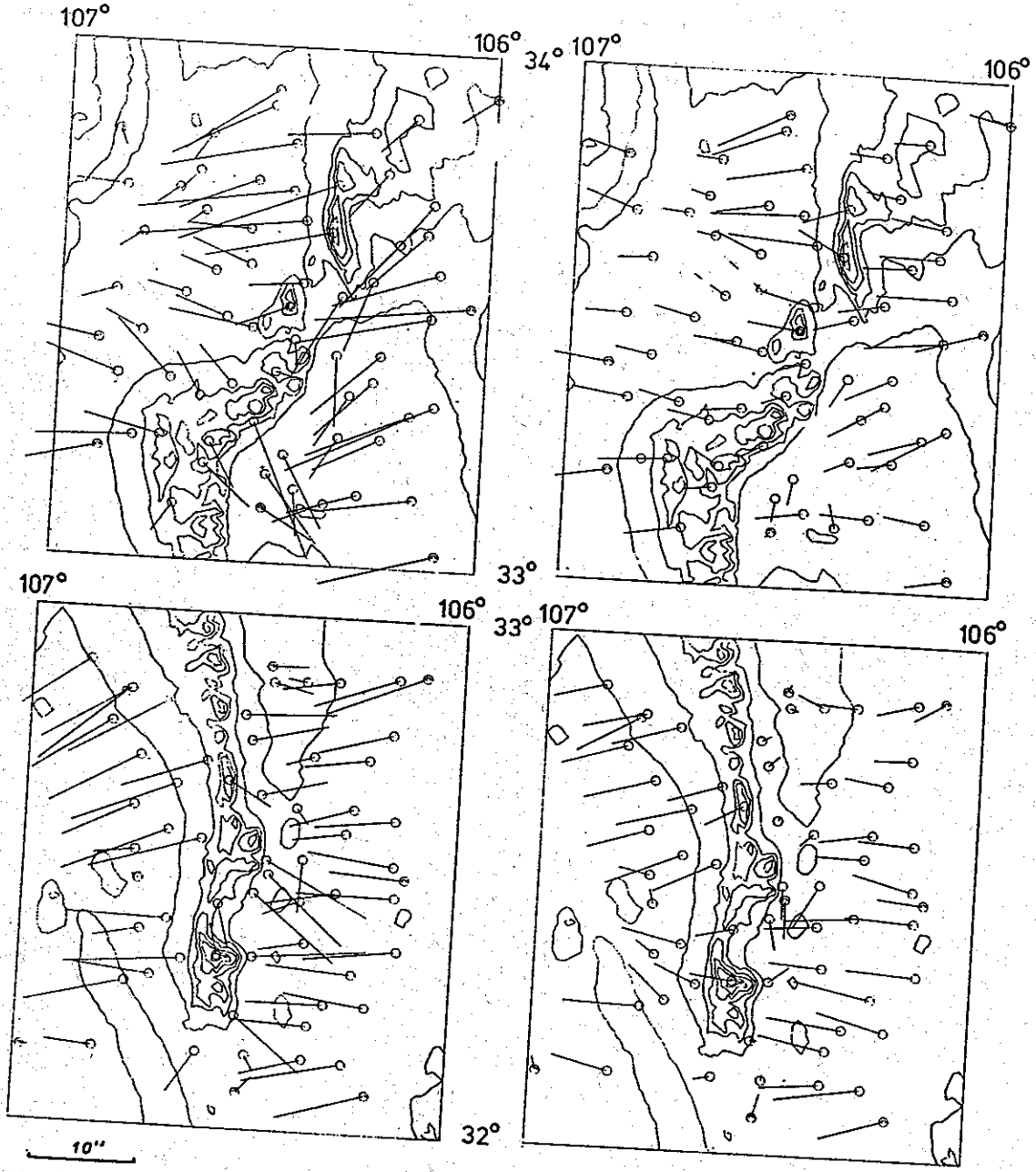

Fig. 10. Observed (left) and terrain-reduced (right) deflections of the vertical. Note the influence of the main mountain chain. Deflections marked with double circles were used as observation data in the 'A' predictions.

New Mexico show that it is possible to predict deflections of the vertical and gravity anomalies with an accuracy of respectively 1 arc sec and 4 mGal from gravity anomalies spaced as far as 6 arc min apart, when the gravity field is smoothed by subtracting terrain effects calculated on the basis of 0.5 × 0.5 arc min point heights. It is thus seen that when appropriate methods are used for accounting for the topography, the method of collocation produces excellent results also in areas of rough topography, the accuracy being similar to the accuracy obtained in lowlands.

TABLE 1. Observed and Terrain-Reduced Deflections and Gravity Anomalies, New Mexico

Terrain Reduction	ξ, arc sec		η, arc sec		Δg, mGal	
	Mean	Standard Deviation	Mean	Standard Deviation	Mean	Standard Deviation
None	−2.11	2.84	−4.43	5.67	−9.95	26.65
ISO	−0.24	1.52	−4.02	2.35	12.06	11.56
TOPO	4.65	2.07	−6.97	2.52	−152.96	12.18
RTM30	−2.03	1.69	−4.56	3.79	−5.73	15.67
RTM15	−2.10	1.87	−4.57	4.25	−7.26	18.37

TABLE 2. Collocation Prediction Results for the Two 1° × 1° Areas, New Mexico

Terrain Reduction	Used Point Observations: A Gravity plus Deflections Mean	A Standard Deviation	B Gravity Alone Mean	B Standard Deviation	C None Mean	C Standard Deviation
None						
ξ	0.30	2.51	−0.07	2.50	−0.19	2.99
η	−0.53	2.58	0.06	2.98	0.68	5.82
Δg	1.24	11.37	1.52	10.48	−2.37	30.67
ISO						
ξ	0.31	0.84	0.25	0.89	0.24	1.48
η	0.00	0.96	0.44	1.13	0.50	2.40
Δg	0.22	3.94	0.24	3.70	−3.39	12.79
RTM30						
ξ	0.13	0.96	−0.20	1.12	−0.26	1.79
η	−0.30	1.00	−0.21	1.13	−0.14	3.36
Δg	0.30	4.37	0.56	3.73	2.68	15.49
RTM15						
ξ	0.18	0.88	−0.10	1.02	0.20	1.54
η	−0.09	1.00	−0.16	1.19	0.85	3.40
Δg	0.23	3.89	0.28	4.09	−0.13	14.36

Prediction based on GEM 10 B, 1° × 1° mean gravity anomalies and the local data indicated.

TABLE 3. Prediction Results ('A') for Varying Parameters in the Topographic/Isostatic Reduction

	ξ, arc sec Mean	ξ Standard Deviation	η, arc sec Mean	η Standard Deviation	Δg, mGal Mean	Δg Standard Deviation
Crustal thickness 24 km	0.30	0.85	−0.01	0.96	0.22	3.97
Crustal thickness 32 km (ISO)	0.31	0.84	0.00	0.96	0.22	3.94
Crustal thickness 40 km	0.32	0.84	0.00	0.96	0.24	3.93
No compensation (TOPO)	0.61	0.92	−0.15	1.13	0.29	4.26
ISO reduction using coarse 5 × 5 arc min mean heights only	0.20	1.37	−0.13	1.42	0.19	4.22

As topographic reduction method, we recommend the RTM method. It has the advantage over the topographic/isostatic reduction methods that a fixed area is unnecessary in the calculations, and because there is no need for any sort of isostatic compensation masses, the calculation is also quicker as fewer prisms are involved in the 'building' of the terrain masses. The densest possible topographic information should be utilized in the terrain effect calculations, corresponding to the well-known fact that the local topography near to the station gives a dominant contribution to the terrain effect. This is especially true when calculating gravity terrain corrections. However, even when rough height data (such as 5 × 5 arc min mean heights) are used, substantial improvements occur in the results. Thus one should always use the terrain reduction concept in mountainous areas even when huge areas or the lack of maps prohibit the construction of reasonably detailed digital terrain models, this being the case in areas such as Greenland. (An example of geoid prediction in Greenland using the presented concepts is given by *Forsberg and Madsen* [1981].)

Acknowledgment. The support of NATO research grant 1378 is gratefully acknowledged.

TABLE 4. Deflection of the Vertical Prediction Results, White Sands Area, New Mexico

Source	Approximation Method	Gravity Field Data	Use of Topographic Data	Number of Predicted Deflection Pairs	rms Error, arc sec ξ	rms Error, arc sec η
This work	stepwise collocation	GEM 10B, 1° × 1° mean anomalies	yes	112	1.5	2.5
		as above plus gravity (spaced 6 arc min) and deflections	yes	112	0.9	1.0
Morrison [1977]	least squares prediction	50 deflections	no	100	1.2	1.4
Schwarz [1978]	Vening-Meinesz	GEM 10 plus all available gravity	yes	441	1.4	2.1
Lachapelle and Mainville [1980]	least squares prediction	GEM 10B	yes	68	2.0	3.4
		GEM 10B plus 10 surrounding deflections	yes	68	1.2	2.1

REFERENCES

Boedecker, G., An economically working method for computing the gravimetric terrain correction, *J. Geophys., 41*, 513–521, 1975.

Ehrismann, W., G. Müller, O. Rosenbach, and N. Sperlich, Topographic reduction of gravity measurements by the aid of digital computers, *Boll. Geofis. Teor. Appl., 8*, 29, 3–20. 1966.

Elmiger, A., Studien über Berechnung von Lotabweichungen aus Massen, Interpolation von Lotabweichungen und Geoidbestimmung in der Schweiz, *Mitt. Inst. Geod. Phot. ETH Zürich, 12*, 1969.

Fisher, I., and P. Wyatt, III, Deflections of the vertical from bathymetric data, in *Proceedings, International Symposium on Application of Marine Geodesy*, Marine Technology Society, Washington, D. C., 1974.

Forsberg, R., The use of digital terrain models in gravimetrical reduction and collocation (in Danish) Mag. Scient. thesis, 180 pp., Univ. of Copenhagen, Copenhagen, 1980.

Forsberg, R., and F. Madsen, Geoid prediction in northern Greenland using collocation and digital terrain models, *Ann. Geophys., 37*, 31–36, 1981.

Gurtner, N., Das geoid in der Schweiz, *Astron. Geod. Arb. Schweiz, SGK, 32*, 1978.

Hammer, S., Terrain corrections for gravimeter stations, *Geophysics, 4*, 184–194, 1939.

Hayford, J. F., and W. Bowie, The effect of topography and isostatic compensation upon the intensity of gravity, *Spec. Publ. 10*, U.S. Coast and Geod. Surv., Washington, D. C., 1912.

Heiskanen, W. A., and H. Moritz, *Physical Geodesy*. W. H. Freeman, San Francisco, Calif., 1967.

Jung, K., *Schwerkraftverfahren in der Angewandten Geophysik*, Akademic Verlag, Leipzig, 1961.

Kärki, P., L. Kivioja, and W. A. Heiskanen, Topographic-isostatic reduction maps for the world for the Hayford zones 18-1, Airy Heiskanen System, $T = 30$ km, *Publ. 35*, Isostat. Inst., Inst. of Appl. Geol., Helsinki, 1961.

Lachapelle, G., A spherical harmonic expansion of the isostatic reduction potential, *Boll. Geod. Sci Affine, 3*, 1975.

Lachapelle, G., and A. Mainville, Evaluation of deflections of the vertical in mountainous areas using a combination of topographic-isostatic and astrogeodetic data, in *Collected Papers 1979*, Geodetic Survey Division, Surveys and Mapping Branch, Ottawa, 1980.

MacMillan, W. D., *Theoretical Mechanics*, vol 2, *The Theory of the Potential*, Dover, New York, 1958.

Moritz, H., *Advanced Physical Geodesy*, Herbert Wichmann Verlag, Karlsruhe, 1980.

Morrison, F., Azimuth-dependent statistic for interpolating geodetic data, *Bull. Geod., 51*, 105–118, 1977.

Schwarz, C. R., Deflection computations for network adjustment in the United States, in *Proceedings of the Second International Symposium on Problems Related to the Redefinition of North American Geodetic Networks*. pp. 91–102, National Ocean Survey, Washington, D. C. 1978.

Tscherning, C. C., A Fortran IV program for the determination of the anomaleous potential using stepwise least squares collacation, *Rep. 212*, Dep. of Geod. Sci., Ohio State Univ., Columbus, 1974.

Tscherning, C. C. A introduction to functional analysis with a view to its applications in approximation theory, in *Approximation Methods of Geodesy*, Herbert Wichmann Verlag, Karlsruhe, 1978*a*.

Tscherning, C. C., A users guide to geopotential approximation by stepwise collocation on the RC4000-computer, *Geod. Inst. Den. Medd., 53*, 1978*b*.

Tscherning, C. C., and R. Forsberg, Prediction of deflections of the vertical, in *Proceeding of the Second International Symposium on Problems Related to the Redefinition of North American Geodetic Networks*, pp. 117–134, National Ocean Survey, Washington, D. C., 1978.

Woolard, G. P., The relation of gravity anomalies to surface elevation, crustal structure and geology, *Res. Rep. Ser. 62-9*, Aeronaut. Chart and Inform. Cent., St. Louis, Mo., 1962.

(Received October 14, 1980;
revised March 10, 1981;
accepted April 2, 1981.)